

Supporting Information

Experimental quantification of electrostatics in X-H $\cdots\pi$ hydrogen bonds

Miguel Saggu,^{1*} Nicholas M. Levinson,^{1*} and Steven G. Boxer^{1*}

¹ Department of Chemistry, Stanford University, Stanford, CA 94305-5012, USA

* To whom correspondence should be addressed. E-mail: miguel.saggu@gmail.com (M.S.),
nickl@stanford.edu (N.M.L.), sboxer@stanford.edu (S.G.B.)

Tables

Table S1. Observed vibrational frequencies for the N-H stretch mode of indole and S-H stretch mode of thiophenol dissolved in different organic solvents at room temperature. The 3rd column shows the frequency shifts relative to the peak of the free species in carbon tetrachloride.

solvent	N-H frequency (cm ⁻¹)	rel. shift (cm ⁻¹)
carbon tetrachloride	3491.5	0
<i>m</i>-dichlorobenzene	3473.8	-17.7
<i>o</i>-dichlorobenzene	3469.6	-21.9
chlorobenzene	3465.4	-26.1
<i>m</i>-fluorotoluene	3451.7	-39.8
benzene	3444.9	-46.6
toluene	3438.7	-52.8
<i>p</i>-xylene	3432.5	-59.0
mesitylene	3425.0	-66.5
1,2,4-trimethylbenzene	3425.4	-66.1
tetramethylbenzene/CCl₄	3420.9	-70.6
pentamethylbenzene/CCl₄	3412.3	-79.3
hexamethylbenzene/CCl₄	3402.6	-87.9

solvent	S-H frequency (cm ⁻¹)	rel. shift (cm ⁻¹)
carbon tetrachloride	2589.0	0
<i>m</i>-dichlorobenzene	2581.0	-8.0
<i>o</i>-dichlorobenzene	2580.6	-8.4
chlorobenzene	2578.7	-10.3
<i>m</i>-fluorotoluene	2574.0	-15.0
benzene	2572.1	-16.9
toluene	2569.9	-19.1
<i>p</i>-xylene	2567.1	-21.9
mesitylene	2562.7	-26.3
1,2,4-trimethylbenzene	2563.0	-26.0
tetramethylbenzene/CCl₄	2559.6	-29.4
pentamethylbenzene/CCl₄	2554.6	-34.4
hexamethylbenzene/CCl₄	2548.8	-40.2

Table S2. Observed vibrational frequencies for the O-H stretch mode of phenol dissolved in different organic solvents at room temperature. The 3rd column shows the frequency shifts relative to the peak of the free species in carbon tetrachloride.

solvent	O-H frequency (cm ⁻¹)	rel. shift (cm ⁻¹)
carbon tetrachloride	3611.0	0
<i>m</i>-dichlorobenzene	3586.1	-24.9
<i>o</i>-dichlorobenzene	3583.4	-27.6
chlorobenzene	3575.8	-35.2
<i>m</i>-fluorotoluene	3568.0	-43.0
benzene	3555.9	-55.1
toluene	3549.6	-61.4
<i>p</i>-xylene	3542.9	-68.1
mesitylene	3534.4	-76.7
1,2,4-trimethylbenzene	3535.0	-76.0
tetramethylbenzene/CCl₄	3526.6	-84.4
pentamethylbenzene/CCl₄	3515.5	-95.1
hexamethylbenzene/CCl₄	3505.2	-105.8

Table S3. Observed vibrational frequencies for the N-H and N-D stretch modes of pyrrol dissolved in different organic solvents at room temperature. The 3rd column shows the frequency shifts relative to the peak of the free species in carbon tetrachloride.

solvent	N-H frequency (cm ⁻¹)	rel. shift (cm ⁻¹)	N-D frequency (cm ⁻¹)	rel. shift (cm ⁻¹)
carbon tetrachloride	3496.2	0	2586.8	0
<i>m</i>-dichlorobenzene	3480.7	-15.5	2576.7	-10.1
<i>o</i>-dichlorobenzene	3477.3	-18.9	2574.7	-12.1
chlorobenzene	3474.3	-21.9	2573.1	-13.7
benzene	3464	-32.2	2569.5	-17.3
toluene	3455	-41.2	2565.1	-21.7
<i>p</i>-xylene	3447.4	-48.8	2560.6	-26.2
mesitylene	3439.8	-56.4	2556.4	-30.4
1,2,4-trimethylbenzene	3442.7	-53.5	2556.7	-30.1
tetramethylbenzene/CCl₄	3433	-63.2	2552.1	-34.7
pentamethylbenzene/CCl₄	3427.1	-69.1	2547.3	-39.5
hexamethylbenzene/CCl₄	3415.7	-80.5	2543.7	-43.1

Figures

Figure S1. Correlation between measured X-H stretch frequencies in different hydrogen bond complexes (in the pure aromatic solvents) and calculated electric fields arising from the aromatic hydrogen bond acceptor based on DFT. (A) Indole N-H $\cdots\pi$ interaction. (B) Thiophenol S-H $\cdots\pi$ interaction.

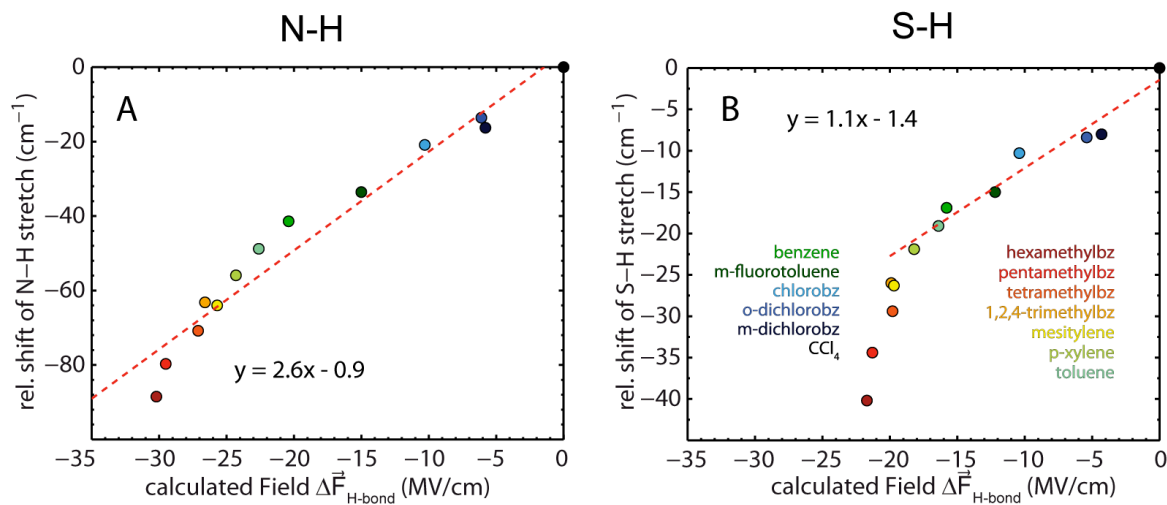


Figure S2. Correlation between measured N-H and N-D stretch frequencies of pyrrole in different hydrogen bond complexes (diluted in CCl_4) and calculated electric fields arising from the aromatic hydrogen bond acceptor based on DFT. The sensitivity of N-D to field is much smaller than N-H, as seen earlier with phenol (O-H vs. O-D).

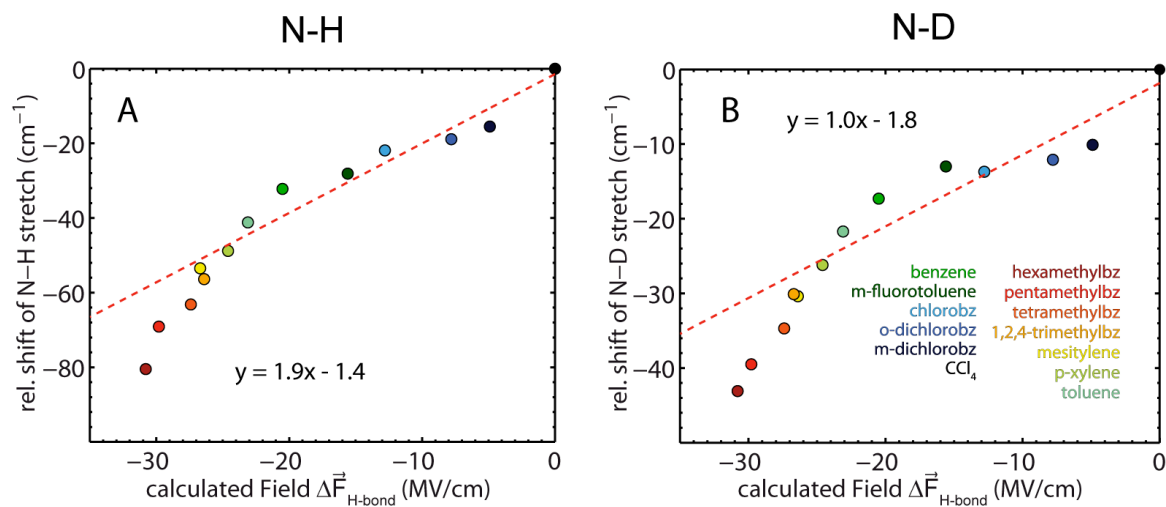


Figure S3. Plot of the vibrational frequencies vs. Onsager solvent reaction fields experienced by indole and thiophenol in the organic solvents. The solvent field (F) was calculated using Onsager's equation below with the dielectric constants of the organic solvents (ϵ) and refractive indices of the solutes (n).¹ The radius (a) used for the spherical solute volumes was calculated from the molar volumes (3.6 Å radius for indole and thiophenol). The dipole moment (μ_0) was 2.11 D for indole and 1.23 D for thiophenol.²

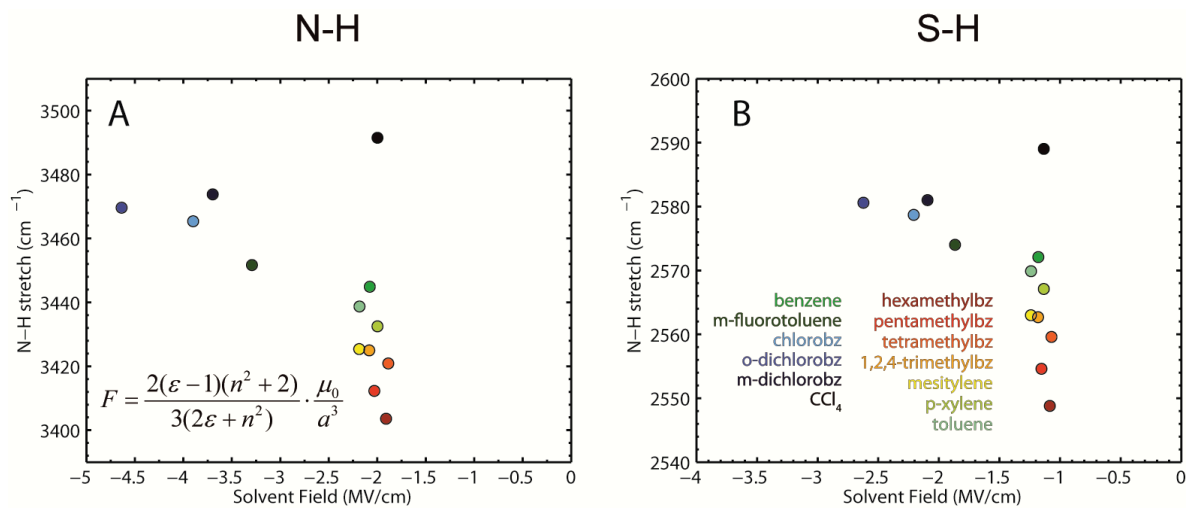


Figure S4. FTIR spectra of 200 mM indole and 200 mM thiophenol in different organic solvents shown without normalization. Intensities of S-H bands increase dramatically in stronger complexes.

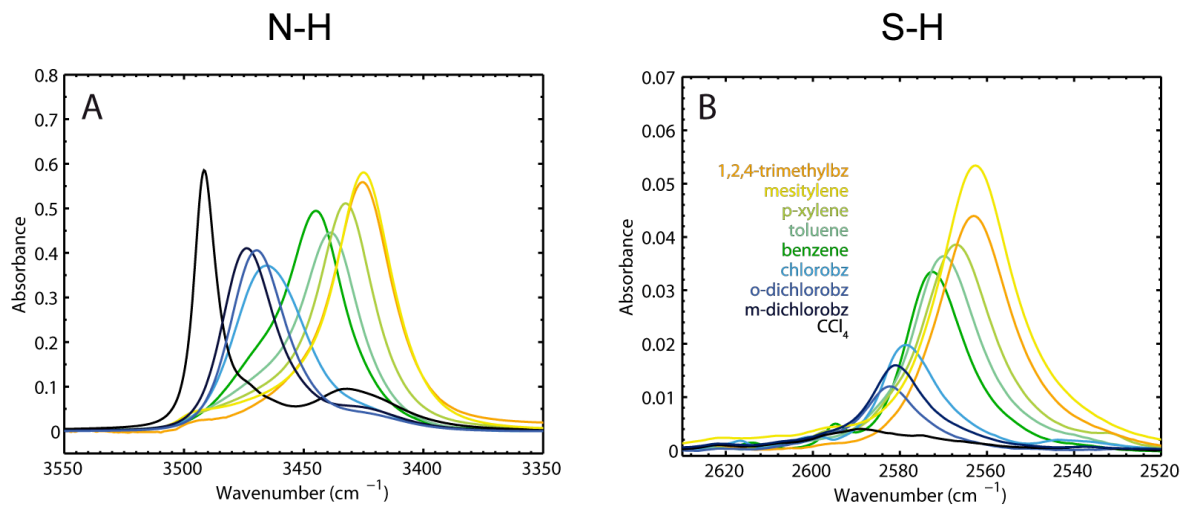


Figure S5. Concentration dependence of the two N-H peaks of indole dissolved in CCl_4 in the room temperature FTIR spectra.

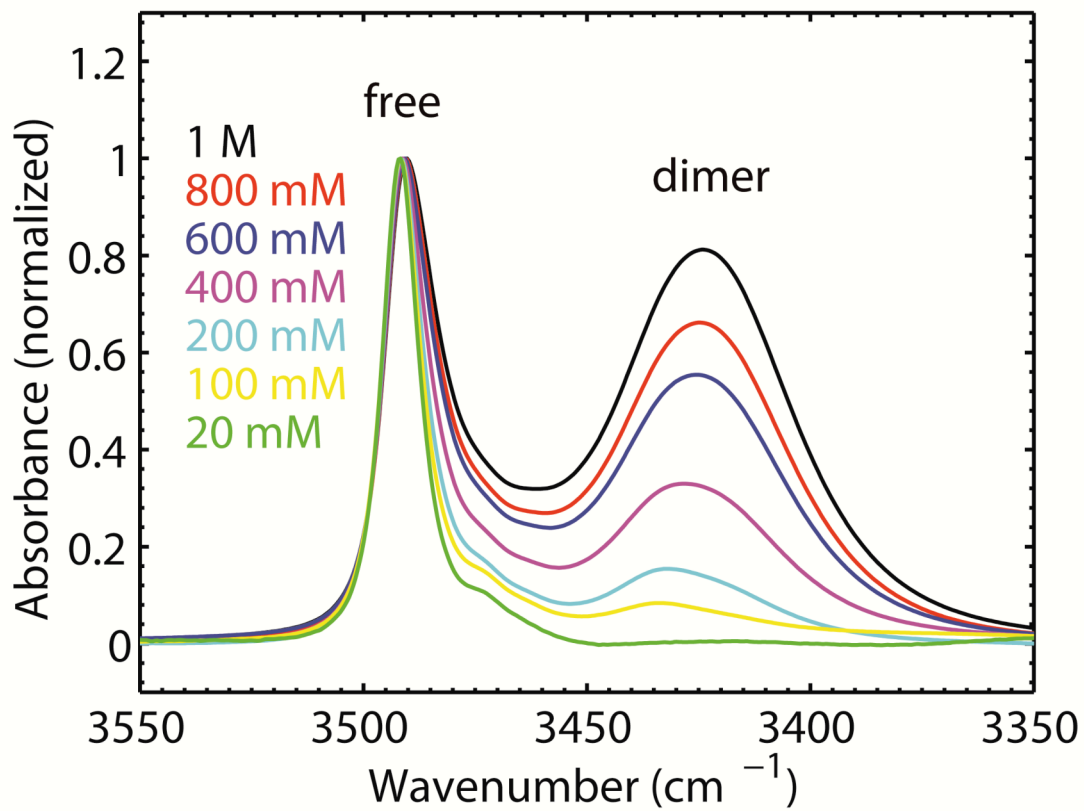


Figure S6. Vibrational Stark spectrum of indole in DCM/DCE recorded at T = 77 K (same data as in Fig. 4B). The Stark spectrum was fitted with the experimentally obtained absorbance spectrum (this includes the assumption of a constant vibrational Stark effect for all chemical species). The Stark tuning rate of the indole:indole dimer is larger than that of the free indole species.

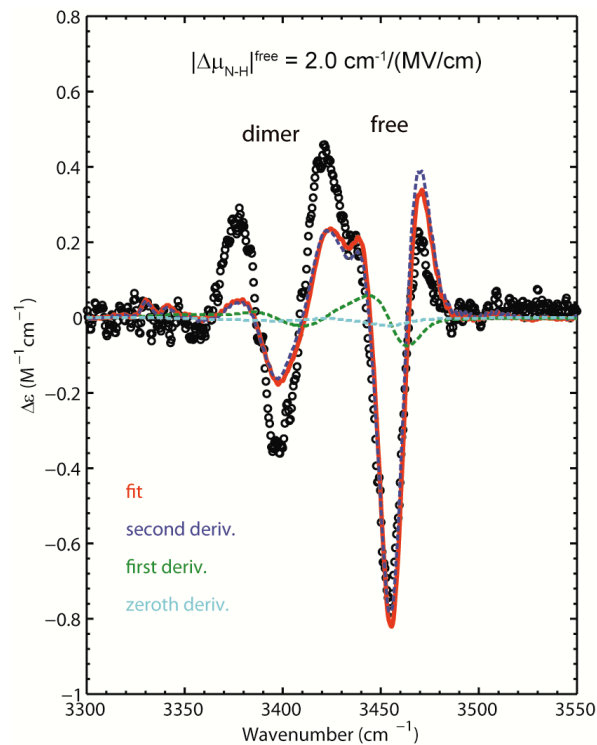


Figure S7. IR extinction and vibrational Stark spectra of indole in different glass-forming solvents recorded at T = 77 K. (A) Extinction spectrum showing the N-H stretch in *m*-fluorotoluene ($\tilde{\nu}_{m\text{-}fluoro} = 3436 \text{ cm}^{-1}$, $\epsilon_{\max} = 82 \text{ M}^{-1}\text{cm}^{-1}$). (B) Stark spectrum scaled to an applied field of 1 MV/cm (dots) with fit (red). (C) Extinction spectrum showing the N-H stretch in butyronitrile ($\tilde{\nu} = 3332 \text{ cm}^{-1}$, $\epsilon_{\max} = 235 \text{ M}^{-1}\text{cm}^{-1}$). (D) Stark spectrum scaled to an applied field of 1 MV/cm (dots) with fit (red).

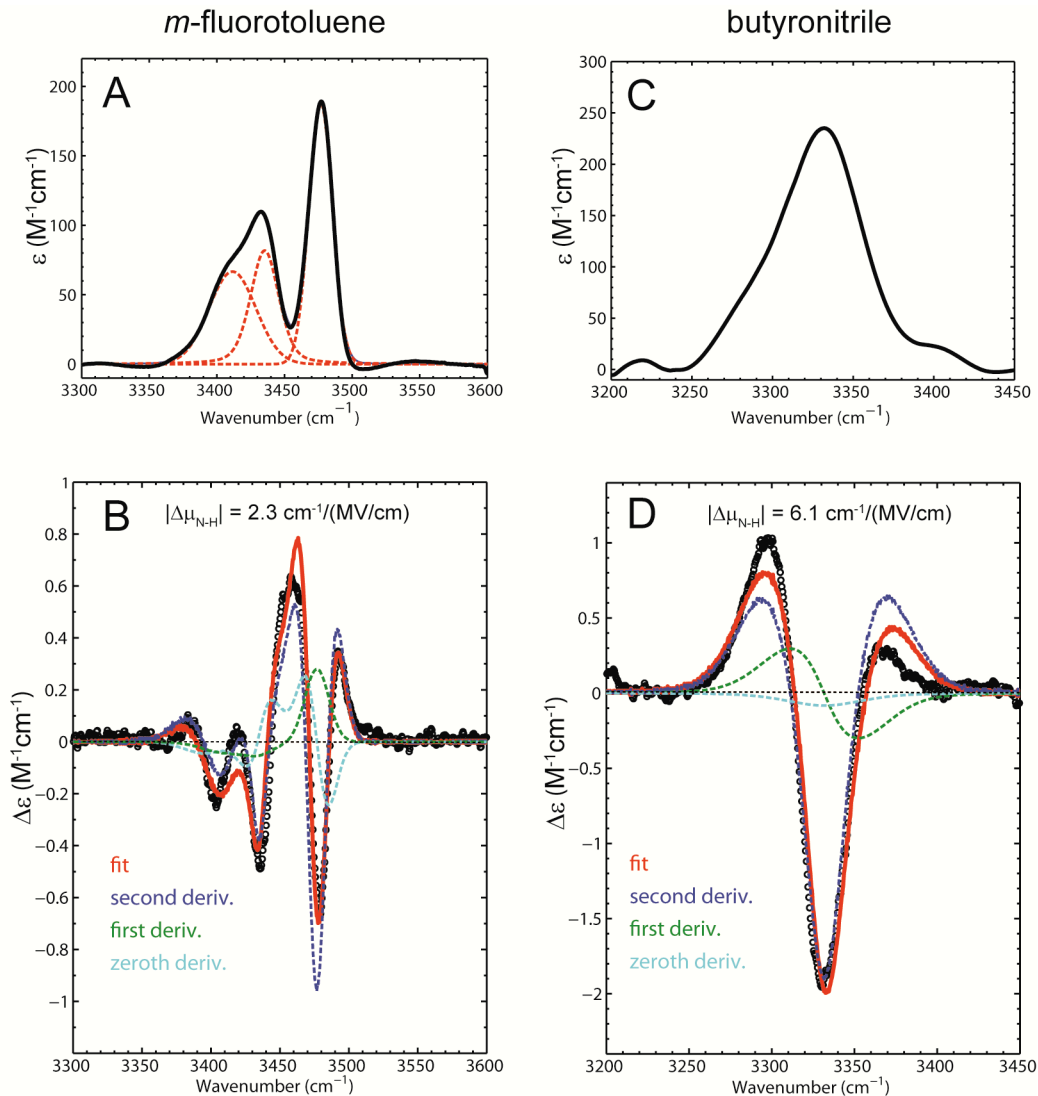


Figure S8. IR extinction and vibrational Stark spectra of thiophenol in different glass-forming solvents recorded at T = 77 K. (A) Extinction spectrum showing the S-H stretch in *m*-fluorotoluene ($\tilde{\nu}_{m\text{-}fluoro} = 2568 \text{ cm}^{-1}$, $\varepsilon_{\max} = 43 \text{ M}^{-1}\text{cm}^{-1}$). (B) Stark spectrum scaled to an applied field of 1 MV/cm (dots) with fit (red). (C) Extinction spectrum showing the S-H stretch in butyronitrile ($\tilde{\nu} = 2546 \text{ cm}^{-1}$, $\varepsilon_{\max} = 128 \text{ M}^{-1}\text{cm}^{-1}$). (D) Stark spectrum scaled to an applied field of 1 MV/cm (dots) with fit (red).

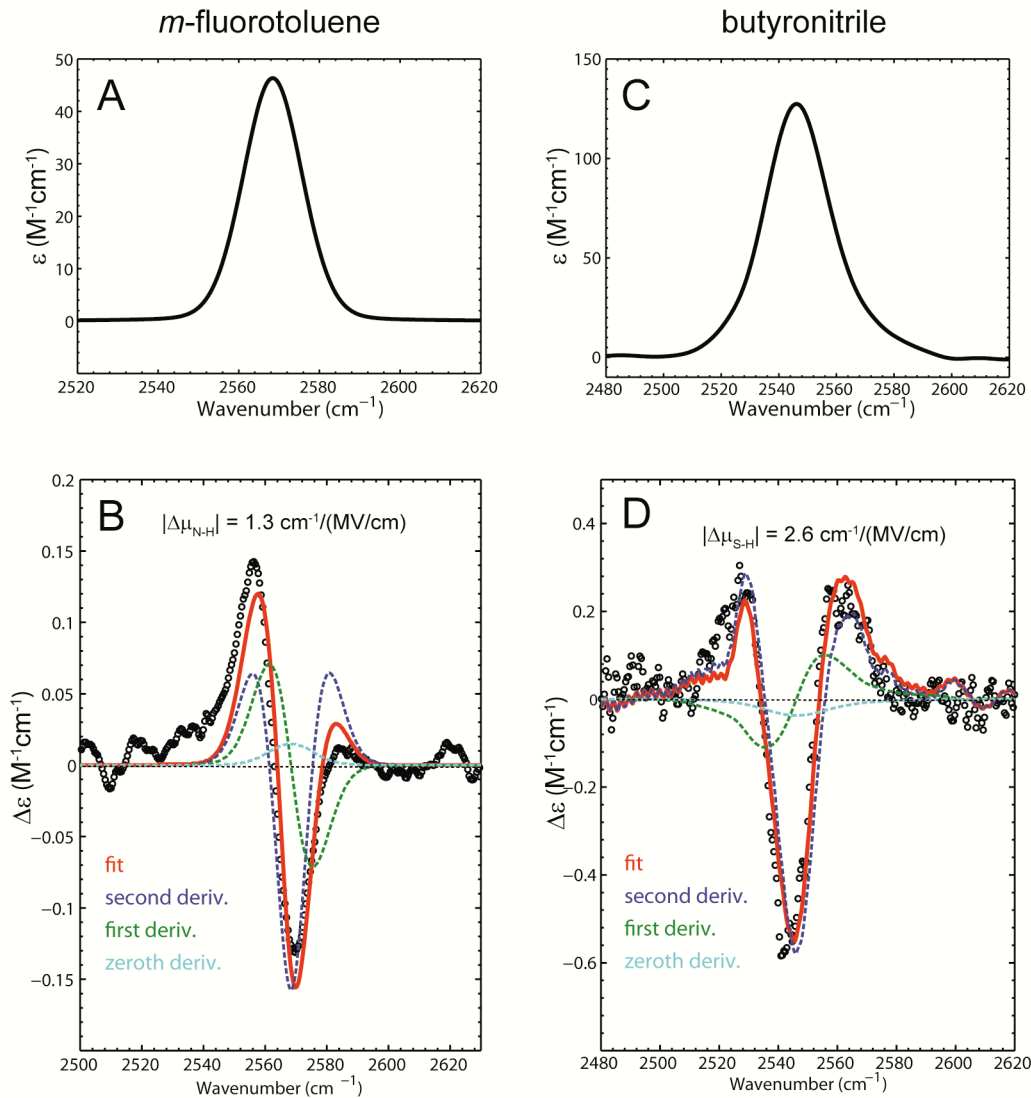
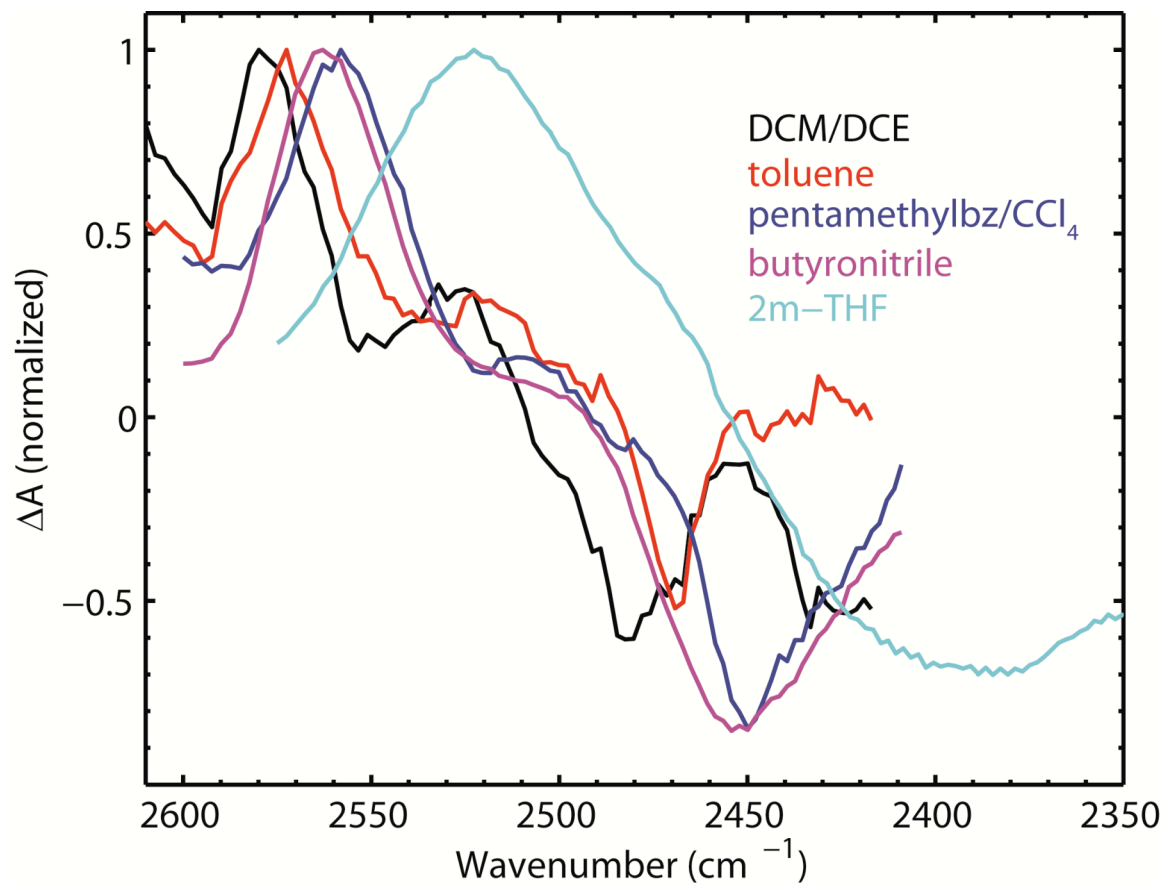


Figure S9. IR pump-probe experiments of thiophenol in different solvents used to determine the anharmonicity of the S-H stretch.



IR pulses were generated using a Ti:Sapphire regeneratively amplified laser/OPA system in which the output of the OPA are 70 fs transform limited 2 μ J IR pulses centered around 2500 cm^{-1} at a 1 kHz repetition rate. The pulses provide a 230 cm^{-1} bandwidth. The light is detected using a 32 element MCT array with a spectral resolution of 2 cm^{-1} . Further details are presented elsewhere.³ The path length of the sample cell was 160 μm and the final OD of the samples was between 0.1 and 0.5.

solvent	anharmonicity $\tilde{\nu}_{0 \rightarrow 1} - \tilde{\nu}_{1 \rightarrow 2}$ (cm^{-1})
DCM/DCE	100 ± 2
toluene	103 ± 2
pentamethylbenzene/CCl ₄	108 ± 2
butyronitrile	109 ± 2
2-methyl-THF	130 ± 10

Calculation of the anharmonic component of the difference dipole

The expectation value of the bond length for a Morse oscillator is given by⁴

$$M_{vv}^{(1)} = \langle v|\hat{r}|v \rangle = \frac{1}{aS} \left[3u + \left(\frac{\frac{7}{2}u^2 + \frac{5}{24}}{S} \right) + \left(\frac{5u^3 + \frac{3u}{4}}{S^2} \right) + \left(\frac{\frac{31}{4}u^4 + \frac{17}{8}u^2 - \frac{23}{960}}{S^3} \right) \right] \quad (4)$$

with

$$a = \sqrt{\frac{k}{2D_e}} \quad S = \sqrt{\frac{8m_{X-H}D_e}{\hbar^2}} \quad u = v + \frac{1}{2} \quad (5)$$

where a is the form parameter of the Morse potential which contains the force constant k of the bond and the dissociation energy D_e , $u = v + 1/2$ where v is the vibrational quantum number and S , a dimensionless parameter, in which m_{X-H} is the reduced mass. The form parameter a and the dimensionless constant S can be calculated from experimentally obtained anharmonicities, which are reported in the literature (102 cm^{-1} for S-H of thiophenol, 136 cm^{-1} for N-H of indole and 160 cm^{-1} for O-H of phenol).⁵⁻⁷ The bond lengthening upon transition from the vibrational ground state to the first excited state is the difference $(M_{11}^{(1)} - M_{00}^{(1)})$.

$$\Delta x = (M_{11}^{(1)} - M_{00}^{(1)}) = \frac{1}{aS} \left[3 + \left(\frac{7}{S} \right) + \left(\frac{17}{S^2} \right) + \left(\frac{43}{S^3} \right) \right] \quad (6)$$

This model predicts a bond lengthening of 0.0331 \AA for O-H, 0.0362 \AA for S-H and 0.032 \AA for N-H for the free species in DCM/DCE.

The difference dipole is then given by the difference in bond length between the vibrational ground state and the first excited state multiplied with the effective charge q of the oscillator obtained from equation 2 according to

$$|\Delta \vec{\mu}_{X-H}^{anh}| = q \cdot \Delta x = q \cdot (M_{11}^{(1)} - M_{00}^{(1)}) \quad (7)$$

From this analysis we obtain the following values:

bond	solvent	Δx (Å)	q (e)	$\Delta\mu^{anh}$ (D)	$\Delta\mu^{exp}$ (D)	$\Delta\mu^{anh}/\Delta\mu^{exp}$
S-H	DCM/DCE	0.0362	0.26	0.0453	0.0654	0.69
	toluene	0.0370	0.29	0.0516	0.0893	0.58
	butyronitrile	0.0384	0.42	0.0780	0.1548	0.50
	2-methyl-THF	0.0434	0.72	0.1510	0.2500	0.60
N-H ^a	DCM/DCE	0.0331	0.70	0.1070	0.1190	0.90
O-H ^b	DCM/DCE	0.0235	0.80	0.1270	0.1369	0.93

^a the anharmonicity is taken from the free indole species in CCl₄

^b the anharmonicity is taken from the free phenol species in the gas-phase

Supporting References

1. Onsager, L. *J. Am. Chem. Soc.* **1936**, *58* , 1486-1493.
2. Lide, D. R. *CRC handbook of chemistry and physics*; CRC Press: Boca Raton, FL, 2005.
3. Steinel, T.; Asbury, J. B.; Zheng, J.; Fayer, M. D. *J. Phys. Chem. A* **2004**, *108* , 10957-10964.
4. Tipping, R. H.; Ogilvie, J. F. *J. Chem. Phys.* **1983**, *79* , 2537-2540.
5. Russell, R. A.; Thompson, H. W. *Proc. R. Soc. London, Ser. A* **1956**, *234* , 318-326.
6. Alencastro, R. B.; Sandorfy, C. *Can. J. Chem.* **1972**, *50* , 3594-3600.
7. Ishiuchi, S. i.; Fujii, M.; Robinson, T. W.; Miller, B. J.; Kjaergaard, H. G. *J. Phys. Chem. A* **2006**, *110* , 7345-7354.

Complete Citation of Reference 28

28. Frisch, M. J.; Trucks, G. W.; Schlegel, H. B.; Scuseria, G. E.; Robb, M. A.; Cheeseman, J. R.; Scalmani, G.; Barone, V.; Mennucci, B.; Petersson, G. A.; Nakatsuji, H.; Caricato, M.; Li, X.; Hratchian, H. P.; Izmaylov, A. F.; Bloino, J.; Zheng, G.; Sonnenberg, J. L.; Hada, M.; Ehara, M.; Toyota, K.; Fukuda, R.; Hasegawa, J.; Ishida, M.; Nakajima, T.; Honda, Y.; Kitao, O.; Nakai, H.; Vreven, T.; Montgomery, J. A.; Peralta, J. E.; Ogliaro, F.; Bearpark, M.; Heyd, J. J.; Brothers, E.; Kudin, K. N.; Staroverov, V. N.; Kobayashi, R.; Normand, J.; Raghavachari, K.; Rendell, A.; Burant, J. C.; Iyengar, S. S.; Tomasi, J.; Cossi, M.; Rega, N.; Millam, J. M.; Klene, M.; Knox, J. E.; Cross, J. B.; Bakken, V.; Adamo, C.; Jaramillo, J.; Gomperts, R.; Stratmann, R. E.; Yazyev, O.; Austin, A. J.; Cammi, R.; Pomelli, C.; Ochterski, J. W.; Martin, R. L.; Morokuma, K.; Zakrzewski, V. G.; Voth, G. A.; Salvador, P.; Dannenberg, J. J.; Dapprich, S.; Daniels, A. D.; Farkas; Foresman, J. B.; Ortiz, J. V.; Cioslowski, J.; Fox, D. J. *Gaussian 09*, Revision A.02. Gaussian, Inc.: Wallingford, CT, 2009.